Chemical Physics Letters 519–520 (2012) 69–72

Contents lists available at SciVerse ScienceDirect

Chemical Physics Letters

journal homepage: www.elsevier.com/locate/cplett

Unravelling the enhanced reactivity of bulk CeO_2 doped with gallium: A periodic DFT study

Paola Quaino [a], Olga Syzgantseva [b,c], Luca Siffert [b,c], Frederik Tielens [d,e], Christian Minot [b,c], Monica Calatayud [b,c,f,*]

[a] PRELINE, Fac. de Ingeniería Química, Universidad Nacional del Litoral, 3000-Santa Fe, Argentina
[b] UPMC Université Paris 06, UMR 7616, Laboratoire de Chimie Théorique, F-75005 Paris, France
[c] CNRS, UMR 7616, Laboratoire de Chimie Théorique, Casier 137, F-75005 Paris, France
[d] UPMC Université Paris 06, UMR 7197, Laboratoire de Réactivité de Surface, Paris, France
[e] CNRS, UMR 7197, Laboratoire de Réactivité de Surface, Casier 178, 4 Place Jussieu, F-75005 Paris, France
[f] Institut Universitaire de France, France

ARTICLE INFO

Article history:
Received 26 September 2011
In final form 9 November 2011
Available online 15 November 2011

ABSTRACT

Doping CeO_2 with gallium leads to promising materials with application in hydrogen purification processes for fuel cells. The bulk ceria–gallia is investigated by *ab initio* calculations. The outstanding reactivity is explained by important relaxations induced by gallium in the ceria host, having a strong impact in the electronic structure. As a result, the mixed oxide is found to be more reducible than the pure oxides in agreement with experimental data. It is thus possible to correlate structure and reactivity of the doped system on the molecular level, representing a step forward to the rational design of materials with selected properties.

1. Introduction

Cerium oxide based materials are among the most important active supports employed in technological applications because of their unique acid–base and redox properties [1]. These properties can be easily tuned by doping the ceria host structure with other cations: Al, La, Zr, etc. [2–8]. The doped materials show enhanced reactivity and are efficient catalysts in selective oxidation reactions; in particular they receive nowadays attention for hydrogen purification processes to feed fuel cells. The role of the dopant is to generate mobile oxygen vacancies in the network structure, as well as to improve different features such as thermal stability and surface area in comparison with pure ceria. Moreover, the presence of metal cations in the ceria lattice can induce formation of specific crystallographic phases for the mixed material. For instance ceria–zirconia systems are found to exhibit outstanding oxygen storage capacities compared with pure ceria [9], as well as highly efficient catalytic properties in selective oxidation reactions [10]. Recently, ceria–gallia catalysts have proven to be as efficient as the commercial ceria–zirconia catalysts in CO catalytic oxidation [11] rendering the mixed oxide promising for the production and purification of hydrogen in fuel cells. Revealing the structure–reactivity relationships on the molecular level is crucial to identify the active sites and to guide the design of materials with selected properties. In this context, the aim of the present Letter is to provide fundamental information on the mixed Ga_2O_3–CeO_2 oxide from an *ab initio* periodic DFT basis. It will be shown that the mixed oxide exhibits unique properties compared with the pure materials, explaining previous experimental results and giving a comprehensive picture of its remarkable reactivity observed in catalytic reactions.

There is little information in the literature regarding mixed ceria/gallia oxides [12–15]. They were successfully synthesized and characterized as regards their structure, chemical composition and chemical reactivity. The Ga^{3+} ions substitute Ce^{4+} cations in the fluorite lattice forming a solid solution for Ga content up to 25%, for higher concentrations in Ga segregation of pure ceria and pure gallia occurs. The samples are more acidic than pure CeO_2 materials [15] and exhibit higher reducibility [13]. Based on the structural information available we present in this Letter a periodic model for the ceria–gallia bulk structure. Geometrical and electronic features are discussed and compared with pure ceria and pure gallia materials, revealing the unique properties of this mixed oxide.

2. Computational details

The VASP package [16,17] was used to carry out all the calculations, with the Perdew–Burke–Ernzernhof PBE functional [18]. The core electrons are kept frozen and replaced by pseudopotentials

* Corresponding author at: UPMC Université Paris 06, UMR 7616, Laboratoire de Chimie Théorique, Casier 137, 4 Place Jussieu, F-75005 Paris, France. Fax: +33 1 44 27 41 17.
E-mail address: calatayu@lct.jussieu.fr (M. Calatayud).

0009-2614/$ - see front matter © 2011 Elsevier B.V. All rights reserved.
doi:10.1016/j.cplett.2011.11.022

generated by the plane augmented wave method PAW. The outshell electrons (Ce: $5s^2\ 5p^6\ 4f^1\ 5d^1\ 6s^2$, O: $2s^2\ 2p^4$, Ga: $3d^{10}\ 4s^2\ 4p^1$) are treated by means of a plane-wave basis set with a cutoff of 350 eV. Distance between k-points in the Brillouin zone is set to $\sim$0.033 $Å^{-1}$ for the optimizations, 0.025 $Å^{-1}$ for the density of states (DOS) calculations. First, the stoichiometric oxides were optimized as regards ion position and volume with the conjugate-gradient algorithm (cutoff set to 420 eV when volume optimization is considered). Then the DOS was calculated for selected optimized structures. Finally, oxygen vacancy formation energy was calculated following Eq. (1) optimizing volume and atomic position. Spin polarization is used when necessary (O_2 molecule, reduced ceria and ceria–gallia models, all have two unpaired electrons).

$$E_f^{1/2O_2} = [E(\text{reduced}) + E(1/2O_2)] - E(\text{stoichiometric}) \quad (1)$$

The unit cells of CeO_2, Ga_2O_3 are depicted in Figure 1, and the optimized bulk parameters are reported in Table 1. Cerium dioxide is cubic, fluorite type, with eightfold coordinated cerium atoms and tetrahedral coordinated oxygen atoms. Ga_2O_3 is represented by the beta-phase, which is the most stable thermodynamically, where gallium is in a distorted octahedral or tetrahedral environment, and oxygen atoms are fourfold or threefold coordinated, respectively. For the mixed phase, a fluorite-type host ($2 \times 2 \times 2$ unit cell) has been considered, since XRD results show only the cubic ceria peaks, indicating that a solid solution is probably present [11–15]. Next, two Ce^{4+} sites are replaced by two Ga^{3+}, and one oxygen is removed in order to keep the ions in their oxidation states Ce^{4+}, Ga^{3+} and O^{2-}. The overall reaction is indicated by Eq. (2):

$$30CeO_2 + Ga_2O_3 = Ce_{30}Ga_2O_{63} \quad (2)$$

The models correspond thus to 6.25% content in gallium. The $Ce_{30}Ga_2O_{63}$ composition corresponds to the stoichiometric oxides; in reduced structures one oxygen atom is removed from the stoichiometric structure and their formula is thus $Ce_{30}Ga_2O_{62}$. The distribution of gallium and oxygen in the network is described below.

Different Ga–Ga relative positions in a ($2 \times 2 \times 2$) fluorite unit cell have been systematically considered and are depicted in Figure 2. Similarly, different positions for the oxygen vacancy have also been investigated in a systematic way: Ga–O–Ga, Ce–O–Ga and Ce–O–Ce sites. The most stable structures always show Ce–O–Ga vacancies, while Ga–O–Ga and Ce–O–Ce vacancies lead to less stable structures, see Figure 1S. As regards the relative Ga–Ga distances, the most favorable situation involves neighboring Ga–Ga sites while isolated Ga sites, which corresponds to long Ga–Ga distances, are higher in energy by about 0.5 eV, see Figure 2.

Table 1
Geometrical parameters obtained for the pure and mixed ceria–gallia materials. Cell parameters in Å; energy (in eV) is given per metal (Ce or Ga) unit in order to compare cells with different metal content.

		Calc.	Exp.
β-Ga_2O_3	a	12.39	12.23 [19]
	b	3.08	3.04
	c	5.87	5.8
	x	0.0903	0.0904
	z	0.7951	0.7948
	E/unit	−30.27	
CeO_2	a	5.460	5.41 [13]
	E/unit	−26.31	
$Ce_{30}Ga_2O_{63}$	a	5.456/5.448[a]	5.37 [13]
	E/unit	−25.49/−25.55[a]	

[a] First value corresponds to isolated Ga sites, second to «pairs», see the text.

The tendency to exhibit gallium sites close to each other is coherent with the endothermic energy found for the formation of the mixed phase, reaction [1] that would indicate a tendency to segregation or the formation of a different crystallographic phase. Experimental X-ray Diffraction (XRD) [13,15] and digital diffraction patterns of High Resolution Transmission Electron Microscopy (HRTEM) observations [11] clearly detect the ceria fluorite phase. Although it is not possible to identify the relative position of gallium sites, such observation would support the formation of a solid solution. The energy difference between neighboring and isolated sites, 0.5 eV for 32 MO_x units, is small enough to be accessible from the thermodynamic point of view considering the working conditions of the catalysts (for example, 523 K and 0.1 MPa for the water gas shift reaction). Moreover, entropy factors may likely favor dispersion. Therefore, we conclude that a realistic model may be the one considering isolated Ga sites. Accurate structural measurements such as Extended X-ray Absorption Fine Structure (EXAFS) and X-ray Absorption Near Edge Structure (XANES) would be needed to get more insight about the local environment and coordination of gallium sites.

The substitution of Ce sites by Ga sites, together with the removal of an oxygen atom to maintain the formal oxidation states, leads to local relaxations around the gallium sites. The relaxation mainly involves the formation of tetrahedral gallium in all cases. Figure 3 shows the structure considering isolated Ga sites (initial Ga–Ga distance 9.37 Å, relative energy 0.56 eV, see Figure 2) which was chosen as representative model.

Starting from pure ceria geometry, the unit cell and the ionic positions are allowed to relax. The initial environment around gallium is that of pure ceria, i.e. cubic with eight equivalent Ga–O

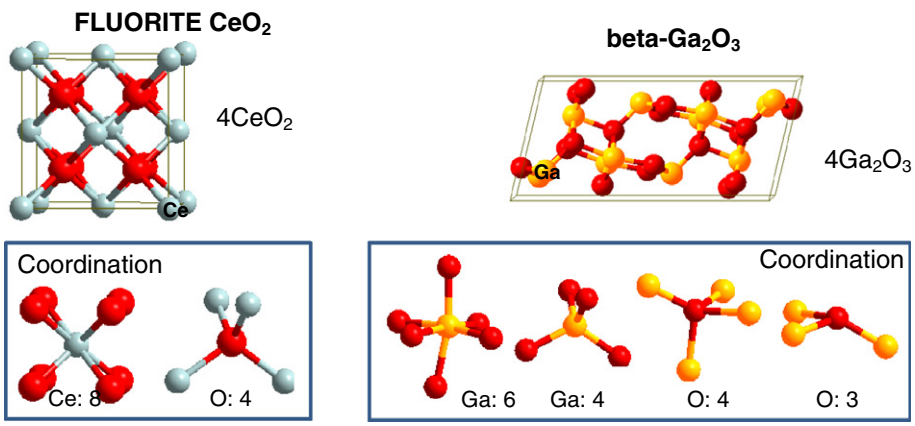

Figure 1. Bulk structures for pure ceria and β-gallia materials.

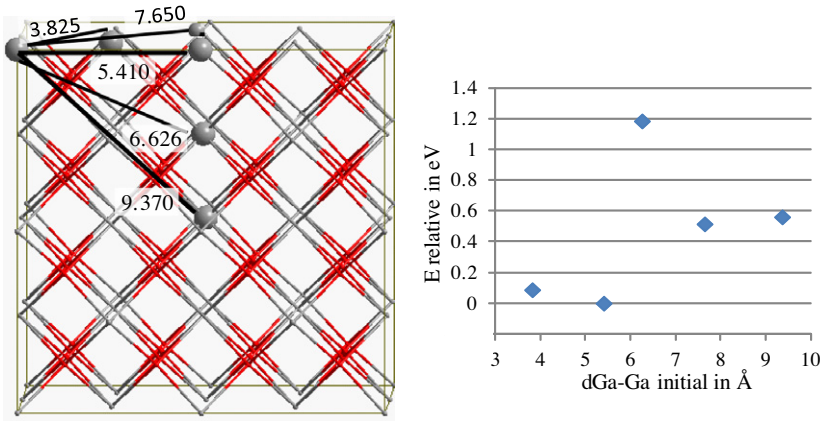

Figure 2. Left, relative Ga–Ga positions in a $(2 \times 2 \times 2)$ fluorite unit cell, distances in Å; right, relative energy for different initial Ga–Ga positions.

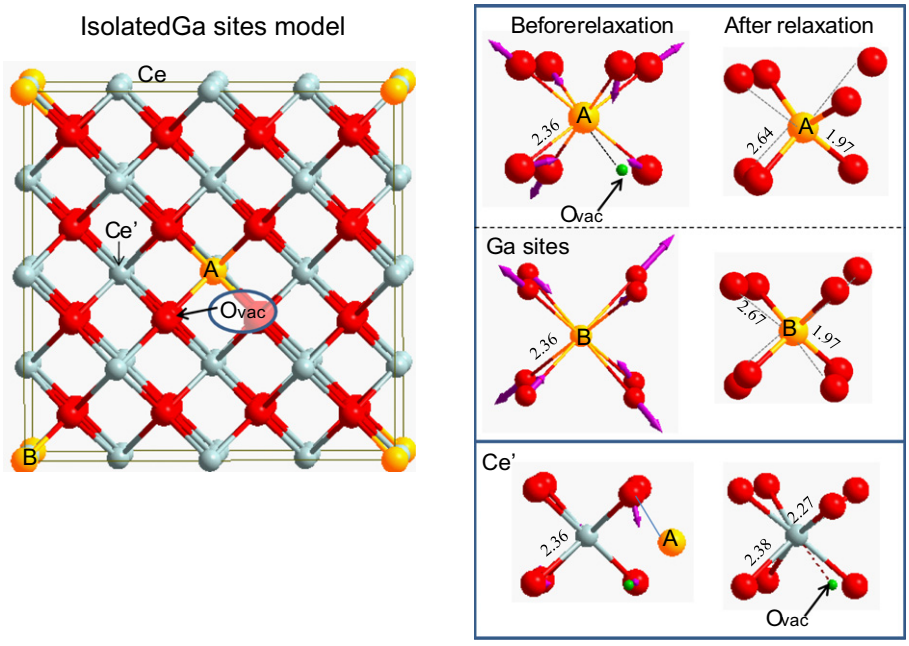

Figure 3. Relaxation effect in geometry for the isolated Ga model: left, starting point; right, local relaxation around selected sites. Arrows indicate how atoms move in the optimization process. Distances in Å.

distances of 2.364 Å. After relaxation, four Ga–O bonds shorten to 1.88–1.93 Å forming a tetrahedron around gallium; the Ga–O bonds left stretch to 2.66–2.67 Å which means they are no longer bonded. For comparison, the Ga–O distances in pure β-gallia for the tetrahedral site are 1.85–1.89 Å, those for the octahedral site are 1.93–2.07 Å. Therefore we conclude that gallium in the ceria matrix is tetrahedral. As regards cerium sites, they become asymmetric cubic with two different Ce–O distances: 2.26–2.28 Å and 2.35–2.40 Å. These features are found in all the structures studied and do not depend on the location of the oxygen vacancy. The removal of an oxygen atom distorts the structure by decreasing the coordination around cerium, but leaves the M–O distances almost unchanged. The cell parameter of the unit cell slightly decreases after relaxation, see Table 1.

The total (DOS) and the *spdf*-projected density of states have been calculated for pure ceria, pure gallia and the mixed structure, and are displayed in Figure 4. In all the oxides the valence band (VB) presents an O-sp character (the highest contribution is given by the 2p O states) and the conduction band (CB) is mainly of metal character: Ce-4f for pure and mixed ceria structures, Ga-sp for pure gallia.

The mixed structures show a DOS profile similar to that of pure ceria. The most striking feature for the mixed oxide is the presence of a sharp sp-peak at −4.8 eV, together with a Ga-d important contribution at −12 eV (not shown). Note that the sharp peak at −4.8 eV originates from the isolation of gallium sites: in the pure gallia structure the gallium sites are close to each other and form a wider band centered at −6 eV (red line, middle panel in Figure 4). In the mixed oxide, the peak at −4.8 eV is mainly composed of gallium s-states, both gallium sites give similar contributions as shown in Figure 2S. Dispersion of gallium in the ceria host lattice causes the band to sharpen due to the lack of interaction with close cation sites, and shifts to higher energies. Additionally, the band gap i.e. the difference in energy between VB and CB, is found to decrease for the mixed oxide compared to both pure gallia and pure ceria, as can be seen in Table 2, Figure 3S.

An important feature of the DOS which is an estimate of the reducibility of the material is the oxygen vacancy formation energy

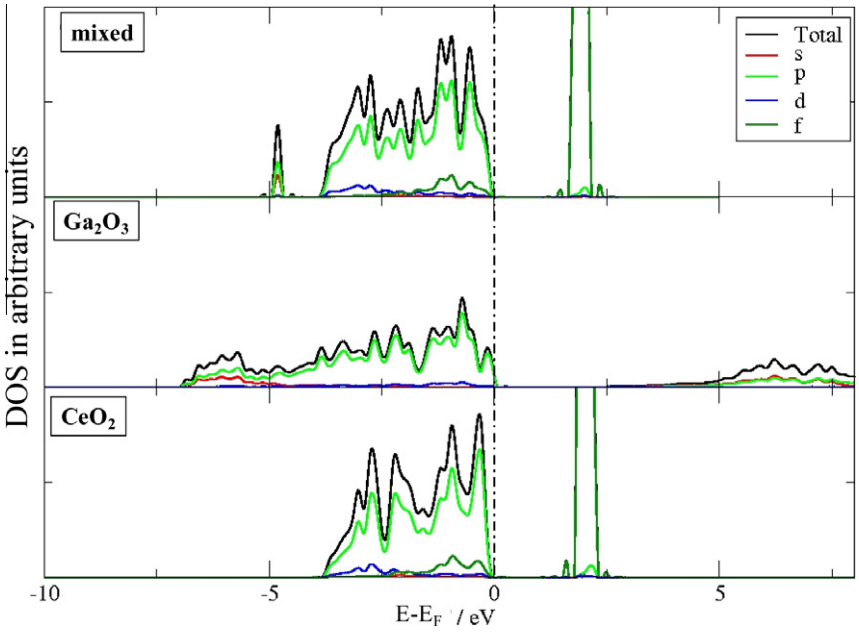

Figure 4. The local density of states (DOS) for the mixed oxide (upper panel), pure gallia (middle) and pure ceria (bottom). The Fermi energy E_F was taken as the zero energy.

Table 2
Band gap (BG) and calculated oxygen vacancy formation energy ($E_f^{1/2O_2}$) for the selected structures, in eV.

	BG calculated	BG experimental	$E_f^{1/2O_2}$
β-Ga_2O_3	2.50	4.9 [20]	4.14[a]
CeO_2	1.80	3.0 [21]	2.95
$Ce_{30}Ga_2O_{63}$ isolated	1.68	Not available	2.37

[a] For a (1 × 3 × 2) unit cell in order to keep similar concentration of vacancies.

$E_f^{1/2O_2}$. It has been calculated for the three materials following Eq. (1) and is reported in Table 2. The lower the (positive) value, the more reducible the material. It is observed in Table 2 that the $E_f^{1/2O_2}$ value for the mixed model (2.37 eV) is lower than pure ceria (2.95 eV) and pure gallia (4.14 eV) thus confirming the enhanced reducibility of the doped material compared to the pure ones.

To summarize, periodic DFT calculations have been performed to characterize the bulk mixed ceria–gallia materials. A 6.25% gallia content model has been constructed from pure ceria fluorite structure. Gallium sites substitute cerium in the structure inducing important local relaxations and decreasing the coordination around the cations in the lattice. Isolated gallium sites significantly alter the electronic structure of the ceria host mainly by decreasing the band gap. In line with this result, oxygen atoms are found to be easily removed from the lattice in the mixed oxide compared to the pure ones, confirming the higher reducibility of the mixed material in agreement with experiments. The geometric relaxations induced by the presence of gallium in the lattice seem to lie at the origin of the enhanced reactivity of the ceria–gallia material.

Acknowledgments

Eulanest 042 CERENH2 and MINCyT-ECOS project A09E01 are gratefully acknowledged for financial support. This work was performed using GENCI-CINES/IDRIS (Grant 2009-[x2009082131], 2010-[x2010082131], 2011-[x2010082022]) and the CCRE-DSI of Université P. M. Curie. P.Q. thanks PICT-0737-2008 and CONICET for continued support. M.C. thanks Institut Universitaire de France IUF for a junior position. Dr. B. Diawara from LCPS ENS Paris is kindly acknowledged for providing us with *ModelView* used in the visualization of the structures.

Appendix A. Supplementary data

Relative energy for the location of the oxygen vacancy; site-projected Density of States for the gallium sites, and comparison of the DOS for the pure and mixed materials. Supplementary data associated with this Letter can be found, in the online version, at doi:10.1016/j.cplett.2011.11.022.

References

[1] A. Trovarelli (Ed.), Catalysis by Ceria and Related Materials, Imperial College Press, London, 2002.
[2] M.F. Luo, Z.L. Yan, L.Y. Jin, J. Mol. Catal. A: Chem. 260 (2006) 157.
[3] B.P. Mandal, V. Grover, A.K. Tyagi, Mater Sci. Eng. A-Struct. Mater. Prop. Microstruct. Process. 430 (2006) 120.
[4] P. Panagiotopoulou, J. Papavasiliou, G. Avgouropoulos, T. Ioannides, D.I. Kondarides, Chem. Eng. J. 134 (2007) 16.
[5] P. Shuk, M. Greenblatt, J. Alloy. Compd. 303 (2000) 465.
[6] X.L. Song, J. Nan, Y.K. Li, D.Y. Xu, J. Rare Earth 25 (2007) 428.
[7] A. Varez, E. Garcia-Gonzalez, J. Jolly, J. Sanz, J. Eur. Ceram. Soc. 27 (2007) 3677.
[8] S. Yamazaki, T. Matsui, T. Ohashi, Y. Arita, Solid State Ionics 136 (2000) 913.
[9] H.F. Wang, Y.L. Guo, G.Z. Lu, P. Hu, Angew. Chem.-Int. Ed. 48 (2009) 8289.
[10] C. Bozo, N. Guilhaume, E. Garbowski, M. Primet, Catal. Today 59 (2000) 33.
[11] J. Vecchietti et al., Top. Catal. 54 (2011) 201.
[12] B. Bonnetot, V. Rakic, T. Yuzhakova, C. Guimon, A. Auroux, Chem. Mater. 20 (2008) 1585.
[13] S. Collins, G. Finos, R. Alcantara, E. del Rio, S. Bernal, A. Bonivardi, Appl. Catal. A: General 388 (2010) 202.
[14] T. Yuzhakova, V. Rakic, C. Guimon, A. Auroux, Chem. Mater. 19 (2007) 2970.
[15] G. Finos, S. Collins, G. Blanco, E. del Río, J.M. Cíes, S. Bernal, A. Bonivardi, in press, Catal. Today, doi:10.1016/j.cattod.2011.04.054.
[16] G. Kresse, J. Hafner, Phys. Rev. B 47 (1993) 558.
[17] G. Kresse, J. Hafner, Phys. Rev. B 49 (1994) 14251.
[18] J.P. Perdew, K. Burke, M. Ernzerhof, Phys. Rev. Lett. 77 (1996) 3865.
[19] B.G. Hyde, S. Andersson, Inorganic Crystal Structures, Wiley & sons, NY, 1989.
[20] M. Orita, H. Ohta, M. Hirano, H. Hosono, Appl. Phys. Lett. 77 (2000) 4166.
[21] Z.X. Yang, T.K. Woo, M. Baudin, K. Hermansson, J. Chem. Phys. 120 (2004) 7741.